

Interpreting character embeddings with perceptual representations: the case of shape, sound, and color

Anonymous ACL submission

Abstract

Character-level information is included in many NLP models, but evaluating the information encoded in character representations is an open issue. We leverage perceptual representations in the form of shape, sound, and color embeddings to investigate their correlation to textual representations in five languages. This cross-lingual analysis shows that textual character representations correlate strongly with sound representations for languages using an alphabetic script, while shape correlates with featural scripts. We further develop a set of probing classifiers to intrinsically evaluate what phonological information is encoded in character embeddings. Our results suggest that information on features such as *voiceness* are embedded in both LSTM and transformer-based representations.

1 Introduction

On the one hand, writing is an essential form of human communication. Writing systems and orthographies differ across languages and impact our reading behavior. Psycholinguists have extensively studied the effect of orthographic depth, i.e., the transparency of grapheme-to-phoneme mappings, on reading acquisition as well as skilled reading (Seymour et al., 2003).

On the other hand, the wide range of cross-linguistic diversity is still a major challenge for natural language processing (NLP) and for the study of language more generally (Mielke et al., 2019; Gutierrez-Vasques and Mijangos, 2020), especially on sub-word levels (Gutierrez-Vasques et al., 2021). This increases the importance of cross-lingual analyses of character-level language models (LMs), because anglocentrism in linguistic research is not only prevalent in NLP, but also in (reading and) orthography research (Share, 2008).

Character-based language models have gained significant attention in recent years in languages

with Latin scripts, since they contain meaningful information on various linguistic levels and enhance the robustness of models. Oh et al. (2021) suggest that character LMs provide a more human-like account of sentence processing, which assumes a larger role of morphology, phonotactics, and orthographic complexity than was previously thought. Moreover, including character and sub-character information in LMs for Asian scripts is a standard practice. Despite of this recent attention, work focusing on getting a deeper understanding of character representation is scarce (Kann and Monsalve-Mercado, 2021), in particular regarding the comparison between languages and different types of scripts.

The goal of this work is to improve our understanding of learned character representations, for better interpretability of the models. Like other neural network based models, character-level LMs can be seen as black-box methods and reveal limited insights about the causes for their predictions (Gilpin et al., 2018). We investigate the information encoded in character embeddings by comparing them to perceptual representations. These representations emerge as an inherent byproduct of human language processing, from reading, writing and speaking. We create embeddings based on the *shape* of characters, the *sound* (phonological features derived from grapheme-to-phoneme mappings) and *color* (elicited in the form of grapheme-color mappings from synesthetes).

Contributions We train models to learn three types of character embeddings: a positive point-wise mutual information (PPMI) vectorization, a recurrent model, and a transformer model. As an intrinsic evaluation method, we analyze the correlations between the distances of textual character representations and the perceptual representations in the form of shape, sound, and color embeddings. Furthermore, to provide more interpretable evalua-

tion methods for character embeddings, we propose a set of probing classifiers to predict phonological features. Crucially, we address the cross-linguistic challenges that arise with character-level modeling by taking into account languages of varying scripts and orthographic depths. We argue that character-level black-box models can only be understood through cross-linguistic approaches and not on individual languages. We perform analyses of five languages: Dutch, English, Japanese, Korean, and Spanish. We discuss the compelling patterns of significant correlations and show the effectiveness of the probing classifiers even in a zero-shot scenario. The implementation and character representations are available online¹.

2 Related Work

Character-level information in LMs. Including character-level information in LMs of languages with Latin scripts has become a common practice in NLP in recent years. This has been the case for different tasks, such as language modeling (Kim et al., 2016; Al-Rfou et al., 2019), part-of-speech tagging (Ling et al., 2015), morphological inflection (Faruqui et al., 2016; Kann and Schütze, 2016; Kann et al., 2020), named entity recognition (Lample et al., 2016), machine translation (Sennrich et al., 2016; Ngo et al., 2019), etc. Character-level information can enhance the models by providing background knowledge in the form of the underlying structures of words in a language (Adouane et al., 2018). Ma et al. (2020) showed how combining character- and word-level information in pre-trained LMs improves not only the performance but also the robustness of the model.

For certain languages, it is standard practice to include sub-token information in LMs, which happens naturally due to the compositional structure of their orthographies. This is the case for East Asian languages such as Korean and Japanese (e.g., Misawa et al. 2017; Chen et al. 2015). Korean LMs are often trained on *Jamos* (i.e., letters, as opposed to syllables), the smallest unit of the Korean script (Ahn et al., 2017; Park et al., 2018). This reduces the vocabulary size and injects syntactic and semantic information to the model that is difficult to access with conventional character- or token-level units (Stratos, 2017). Recently, Lee et al. (2020b) showed that a Korean BERT model using sub-character information requires less train-

ing data than previous models. Similarly, Japanese LMs also benefit from sub-character information (Nguyen et al., 2017).

Evaluating character embeddings. Character-based language models are most often evaluated on downstream NLP tasks or on next character or word prediction (e.g., Takase et al. 2019; Tay et al. 2021; Clark et al. 2021). Additionally, they can be evaluated on word-level intrinsic evaluation tasks such as word analogy or similarity (e.g., Li et al. 2015). While work on intrinsic evaluation of character embeddings is scarce (Kann and Monsalve-Mercado, 2021), the evaluation of neural representation trained on phonemes have received more attention, focusing on what phonological knowledge is embedded within (Silfverberg et al., 2018; Kolachina and Magyar, 2019; Mayer and Nelson, 2020; Mayer, 2020; Silfverberg et al., 2021). In Mayer (2020); Mayer and Nelson (2020) they use characters as an approximation of phonemes in the case of Samoa and Finnish, respectively, as graphemes are closely connected to phonemes in these orthographies. However, this is far from the general trend.

Impact of different orthographies on linguistics and human language learning. Orthographic depth, i.e., the transparency of grapheme-phoneme correspondences in written alphabetic language (Frost et al., 1987; Katz and Frost, 1992), is a well-studied factor influencing reading acquisition and skilled reading behavior (Seymour et al., 2003; Landerl et al., 2013; Richlan, 2020). For instance, English is considered to be a *deep orthography*, as there are often multiple different pronunciations for the same spelling patterns (e.g., <gh> in *tough* and *though*). This contrasts *shallow orthographies* with more reliable grapheme-phoneme correspondences, such as Spanish. The consistency and complexity with which print reflects speech is one of the prime factors of cross-linguistic differences in reading fluency (Ziegler et al., 2010; Schmalz et al., 2015). It is the starting point for any discussion that centers on reading development across languages (Papadopoulos et al., 2021). Since the orthography has such a high impact on human reading behavior, its effect should also be considered more carefully in the development of NLP models.

Impact of different orthographies on NLP models. While orthographic depth has been discussed at length in reading research and psychology, it has

¹Link omitted to preserve anonymity.

rarely been addressed in natural language processing. This partly due to the prevalent anglocentrism and missing resources (Bender, 2018). Some research has gone into studying the differences between languages when it comes to train computational LMs (Mielke et al., 2019), showing the impact of the vocabulary size and sentence length, but there is lack of NLP research analyzing or taking into account the varying orthographies across languages. Two notable exceptions are the recent methods proposed by Marjou (2021) and Sproat and Gutkin (2021), who use neural networks to estimate the transparency of orthographies and degree of logography, respectively. Moreover, Gorman et al. (2020) conducted a shared task on grapheme-to-phoneme prediction. Their results show an urgency for improving these systems and the pronunciation dictionaries used to train them across languages and scripts.

3 Character Representations

3.1 Character language models

We use the Wiki40B multilingual dataset (Guo et al., 2020) to train the character models. For each of the five languages, English (en), Dutch (nl), Spanish (es), Korean (ko), and Japanese (ja), we extract training sets of 3 million characters. The first three languages all use variants of the *Latin* script, while *Hangul* (Korean) and *Hiragana* (one of several scripts used in Japanese) are *syllabary* scripts, in which most graphemes denote entire syllables. We preprocess Korean *Hangul* characters, decomposing them into constituent *Jamos*, each corresponding roughly to a single phoneme. For Japanese, we train the language model on *Hiragana* and *Katakana* characters, but remove *Kanji* symbols to reduce the vocabulary size. The correlation analyses are then only performed on *Hiragana*. Figure 1 shows 2-dimensional plots of the learned textual character representations.

Count-based PPMI embeddings. We generate vectorized character representations in a purely count-based manner with a positive pointwise mutual information (PPMI) weighting. While the importance of positional information is less obvious for modelling word semantics, it is crucial for modelling the distribution of sounds. Following the approach by Mayer (2020), we let our PPMI weighting diverge from traditional bag-of-words models by distinguishing contexts by their relative position

to a target. Thus, embeddings will have independent values for the contexts $AB_$, $_AB$, and A_B , counting the number of times a target proceeds, precedes and mediates a string AB . Using bigram contexts, the resulting embeddings have a dimension of $3 \cdot c^2$, where c is the number of characters in a given language, and 3 indicating the number of possible relative positions.

LSTM. We train a recurrent language model consisting of a unidirectional long-short term memory (LSTM) layer. It receives character sequences as input at each time step and is trained for next character prediction. The model is trained with an Adam optimizer (Kingma and Ba, 2015), an initial learning rate of 0.01, and a batch size of 128. We extract the hidden representations of 128 dimensions as character embeddings. See Appendix C for training specifications.

Transformer. Similarly, we also train a transformer character model on the same data (Vaswani et al., 2017). The input layer consists of character and positional embeddings, followed by a transformer block with 2 heads and a hidden layer size of 128. We follow the same training procedure as for the LSTM.

3.2 Perceptual representations

Sound. The first perceptual representation that we consider is *sound*. To retrieve this representation, we map characters to a phonological distinctive feature space. This method has previously been applied to phonemes as a means of generalisation compared to sparse representations (Rumelhart and McClelland, 1986; Mirea and Bicknell, 2019), and to evaluate the knowledge embedded representations learned from neural networks (Silfverberg et al., 2018; Kolachina and Magyar, 2019).

As sound and speech are only indirectly reflected in writing, we approximate sound representations of characters using grapheme-to-phoneme alignment: For all languages, we extract data from the WikiPron pronunciation dictionary (Lee et al., 2020a) and use the *m2m-aligner* (Jiampojarn et al., 2007) to align graphemes with phonemes in an unsupervised manner. Having alignments from the WikiPron data, we chose the most frequent word-initial phoneme mapping to represent the sound of each character (resulting mappings are listed in the Appendix D). Having a phoneme mapped with to character, we are able to associate it with a set of phonological distinctive

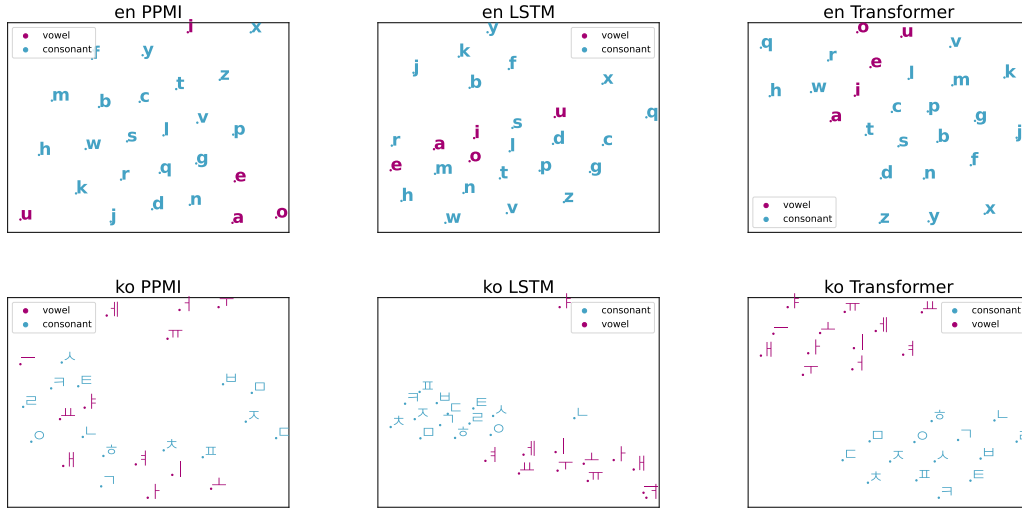


Figure 1: tSNE cluster plots of the character distances from the three types of character language models for English and Korean (see Appendix Figure 6 for the plots for Dutch, Spanish and Japanese).



Figure 2: Example of letter-color associations from single subjects.

features, which we use to form our final sound representation: Using the `ipapy`² toolkit, we retrieve International Phonetic Alphabet (IPA) descriptions of the phoneme mappings from which we create a sparse vector that describes what phonological features (e.g., consonant manner of articulation, \pm plosive, or vowel height, \pm front) are active. For every language, this provides us with a sound embedding table, $S^{|V| \times |F|}$, where V is the set of characters and F is the set of distinctive features, and

$$S_{i,j} = \begin{cases} 1 & \text{if } F_j \in \text{phonmap}(V_i). \\ 0 & \text{otherwise.} \end{cases}$$

Color. Inspired by Kann and Monsalve-Mercado (2021), we compute color character representations from synesthesia data. Grapheme-color synesthe-

sia is a neurological phenomenon in which viewing a grapheme elicits an automatic, involuntary, and consistent sensation of color (Eagleman et al., 2007). Color-to-letter associations in synesthesia allow to examine the relationships between visual, acoustic, and semantic aspects of language. Recent research in this area has found cross-linguistic similarities in synesthesia, suggesting that some influences on grapheme-color associations in synesthesia might be universal and highlighting the importance of multilingual analyses (Root et al., 2018). Figure 2 shows example grapheme-color associations from individual subjects for each of our studied languages. It emphasizes the preference for red color tones for the first letter of the alphabet irrespective of the language (Root et al., 2018).

We use the cross-linguistic synesthesia data collected by Root et al. 2018 (see Appendix B for the dataset statistics). In order to extract color representations we compute the Euclidean distances between the 3-dimensional CIELuv color coding scheme for all character combinations. We average the distances across all participants of the same language. The resulting vector representations reflect the finding of Root et al. (2018) that the first grapheme in any language is unusually distinct (see Figure 5 in Appendix).

Shape. Lastly, we also create simple character representations based on their shape. Previous works (Brang et al., 2011; Watson et al., 2012) have relied on Gibson (1969) or Courrieu et al. (2004) to build shape-related embeddings

²<https://github.com/pettarin/ipapy>

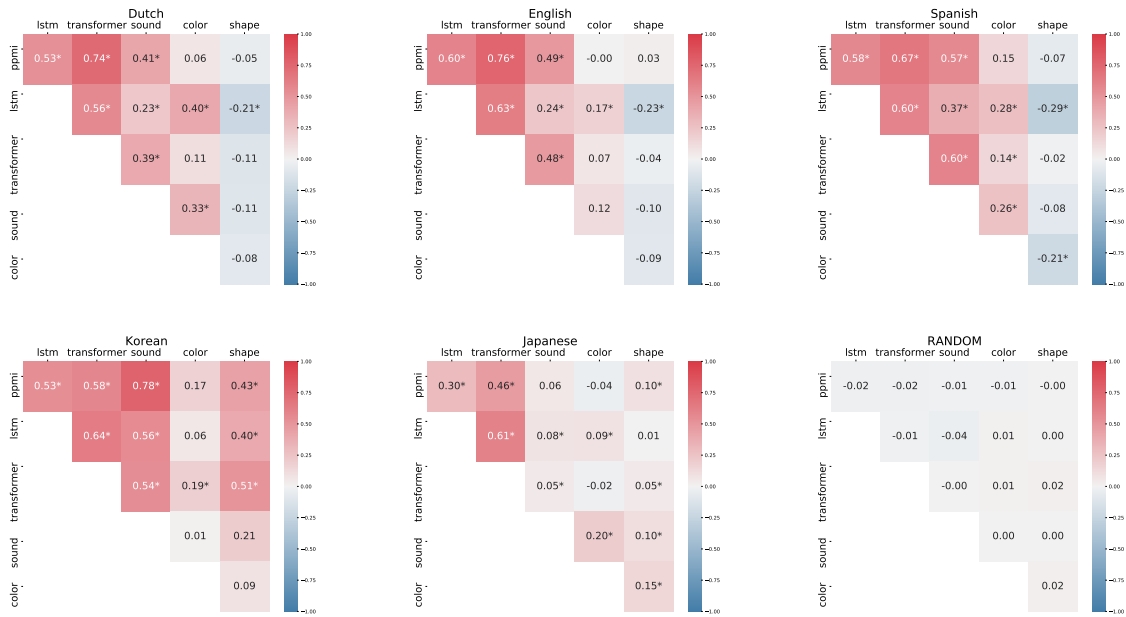


Figure 3: Pearson correlation between all representations types for all five languages and for the random baseline (bottom right). A * marks a significant correlation ($p < 0.01$).

from human similarity judgements. However, we create shape embeddings directly from their visual expressions. We create an image for each printed character as shown in Figure 7 in the appendix. For each script, all images have the same width and height (the largest width among all characters incremented with 10 pixels, and the same for the height, which results approximately in 35×45 pixels) and all characters are drawn at position $\{5, 5\}$. We use the font *Arial Unicode MS* with size 28. From these images, we create shape representations by reading the images as gray scale images from top to bottom and flattening the matrix into vectors.

4 Correlation Analysis

In order to analyze the relation between the learned character representations and the three perceptual representations – sound, shape, and color – we first compute the pairwise distances between characters³. Figure 3 shows the Pearson correlations between the character distances of all embedding types. The figure also includes a baseline, where the correlation between random distances and the distances of the respective character representations is computed.

As expected, the textual character representations show high correlation amongst each other for

³We use cosine distance for all textual, sound and shape representations; and Euclidean distance for color.

all five languages. The correlations between the textual embeddings and the perceptual representations show that even though the first are purely trained on written language, they still learn to encode certain inherent characteristics of human language processing and production:

As a general pattern, the textual character representations correlate strongly with sound representations, moderately with color representations, and not at all with the shape representations (with the exception of Korean, discussed below). Japanese character embeddings behave differently. For instance, the correlation with the sound representations is weaker than for the other languages, which might be due to the syllabic nature of the Japanese script. In the following, we discuss the results for each of the perceptual embedding types in detail.

Sound. The PPMI character embeddings show the highest correlation with sound representations, followed closely by transformer embeddings. This is notable in the three languages with Latin scripts (en, es, nl). To explain this finding, we speculate that the context and learning direction available to the LMs provide phonetic information. Both the PPMI and transformer embeddings learn from context and from positional information in both directions. However, the unidirectional LSTM learns from left-to-right only. Therefore, as an addition, we trained a bidirectional LSTM to show that the

	en	es	nl
LSTM	0.24	0.37	0.23
biLSTM	0.37	0.37	0.30
Transformer	0.48	0.60	0.39
PPMI	0.49	0.57	0.41

Table 1: Correlations between sound representations and character embeddings.

	syllables	Jamos
IPA	0.10*	0.56*
Color	–	0.06
Shape	0.30*	0.40*

Table 2: Pearson correlation coefficients for Korean character embeddings based on Hangul syllables vs. Jamos. As the synesthesia data only includes Jamos, we exclude the syllable correlation for color.

addition of right-to-left information improves the correlation to the sound representations. The results are shown in Table 1. Moreover, comparing the results across Latin script, we note that Spanish character embeddings from all models achieve higher correlations than Dutch and English. The shallow orthography of the Spanish language explains this finding. This is also the case for Korean.

Color. Our findings on the correlation between English character embeddings and synesthesia data are in line with (Kann and Monsalve-Mercado, 2021), who find that LSTMs agree with human letter-color perceptions more than transformers on a dataset with more participants (0.08 for LSTM-LM and 0.0 for transformer-LM). Moreover, we reach the same conclusion for the other alphabetic languages, Dutch and Spanish, while for Korean and Japanese there is no clear pattern evident from the correlation coefficients. This might be due to the smaller number of synesthete participants in the dataset.

Shape. The character embeddings of non-featural Latin scripts show low (or even negative) correlation to the shape embedding. However, due to their featural writing systems (Sampson, 1985; Marjou, 2021), Japanese and especially Korean embeddings correlate significantly with shape. The fact that the Korean consonant graphemes were designed to resemble the place of articulation (Lee, 2021; Gale, 1912), can explain the high correlations between character and shape embeddings for this language.

This is also shown in the positive correlation between sound and shape representations, which is absent for the other languages. To analyze this

further, we compare our initial results with character representations computed based on *Jamos* (e.g., individual phonemes such as \neg), to character representations of full *Hangul* characters (e.g., syllables such as $\frac{\neg}{\text{ㅇ}}$). Table 2 shows higher correlations for characters decomposed into Jamos.

In this light, the result is unsurprising and can be interpreted as an effective proof-of-concept of using a correlation analysis between textual and perceptual representations. More genuine shape representations, for example learned by a convolutional neural network, could be applied to reveal more accurate correlation patterns for Latin scripts.

5 Probing Classifiers

Except for Japanese, the results show that the neural embeddings correlate the most with the perceptual sound representations. To get a closer look at what information that may be encoded in the dense embeddings, we design a probing task in which classifiers are trained to predict whether certain distinctive features are present given character embeddings as input.

5.1 Classifier Setup

For each distinctive feature, we train a binary Logistic Regression to predict whether the feature is present (1), or not (0). The labels are given by the sound representations as explained in Section 3.2. As the number of samples is small (limited to the number of characters in a language), we do this in a leave-one-out manner, training a classifier for each character, while using the rest for training. For features that only concern consonants (e.g., *manner of articulation* and *voiceness*), we exclude vowels, and similarly, for features that only concern vowels (e.g., *vowel height* and *vowel rounding*), we exclude consonants in both test and training.

5.2 Zero-shot classifiers

For some features, choosing the most frequent label is a good strategy and will provide good results. To further challenge the knowledge learned by the embeddings and distinguish the classifiers from the strategy of choosing the most frequent baseline, we create a zero-shot setup in which the classifiers will have to be able to transfer knowledge between features in order to excel in the task. In particular, we test 1) if a classifier trained to predict whether a consonant is voiced is able to identify vowels and 2) if labial consonants are retrieved by a classifier

Model	global type		consonant voiceness		vowel roundness		
	<i>consonant</i>	<i>vowel</i>	<i>voiced</i>	<i>voiceless</i>	<i>rounded</i>	<i>unrounded</i>	
en	LSTM	0.84	0.22	0.67	0.17	-	-
	Transformer	0.90	0.60	0.86	0.71	-	-
	Random	0.61	0.28	0.54	0.43	-	-
	Most-frequent	0.89	0.00	0.76	0.00	-	-
es	LSTM	0.91	0.50	0.57	0.61	0.00	0.57
	Transformer	0.98	0.89	0.72	0.63	0.00	0.33
	Random	0.61	0.27	0.49	0.49	0.43	0.49
	Most-frequent	0.90	0.00	0.00	0.00	0.00	0.00
ko	LSTM	1.00	1.00	0.00	0.88	0.00	0.83
	Transformer	1.00	1.00	0.33	0.87	0.00	0.83
	Random	0.59	0.35	0.29	0.60	0.35	0.56
	Most-frequent	0.84	0.00	0.00	0.88	0.00	0.83
nl	LSTM	0.91	0.50	0.62	0.15	0.00	0.33
	Transformer	0.93	0.67	0.79	0.57	0.00	0.57
	Random	0.61	0.28	0.54	0.42	0.43	0.51
	Most-frequent	0.89	0.00	0.76	0.00	0.00	0.00

Table 3: F1 score for classifiers predicting distinctive features with character embeddings (LSTM, Transformer) as input. Two baselines are included: Random (predicting labels uniformly at random) and Most-frequent (always predicting the most frequent label). Since English only has one rounded vowel (the character 'o' mapped to IPA 'ɒ'), the result for this classifier is not included. Results for predicting all distinctive features are found in Appendix E.

trained to predict vowel rounding. While the intuition behind 1) relates to the sonority sequencing principle, which states that the nucleus of a syllable (vowels in the majority of the cases) represents a sonority peak, the intuition behind 2) is more experimental, relying on a global feature such as 'rounding'.

5.3 Results and discussion

The results for the probing classifiers are found in Table 3. Generally, both LSTM and transformer embeddings outperform both the most-frequent and random baselines, with the transformer beating the LSTM by a small margin. This should, however, be taken with a grain of salt considering the limited number of examples.

Considering the global features, *vowel* and *consonant*, classifiers are able to learn this distinction using both LSTM and transformer character embeddings. In particular, consonants are identified with high certainty. This is, however, the majority group (ref. the most frequent strategy). The F1 scores for vowel prediction are considerably lower. However, in this case they cannot be explained by neither a most-frequent strategy nor a random baseline, which indicates that knowledge about this distinction is present in the embeddings.

The findings for the voiced/voiceless consonant

Model	consonant voiceness:voiced → global type:vowel	
en	LSTM	1.00
	Transformer	1.00
	Random	0.63
	Most-frequent	1.00
es	LSTM	0.89
	Transformer	0.89
	Random	0.64
	Most-frequent	0.00
ko	LSTM	0.44
	Transformer	0.00
	Random	0.65
	Most-frequent	0.00
nl	LSTM	1.00
	Transformer	1.00
	Random	0.63
	Most-frequent	1.00

Table 4: F1 score for predicting vowels using a classifier trained to predict whether a consonant is voiced. Two baselines are included: Random (predicting labels uniformly at random) and Most-frequent (predicting the most-frequent label, w.r.t. the label distribution in the original task).

distinction are similar. But here the groups are more balanced, which provides the most-frequent strategy with less of an advantage and in turn the F1 scores are generally lower. For Korean, the scores are lower compared to the other languages. As the feature of consonant voiceness correlates with manner in Korean (with all plosives, affricates and frica-

Language	F1	True positive	False positive	False negative
es	0.3	m v	t r z	b p f w
nl	0.5	b f v w	k g d q z x	p m
ko	0.4	ㅁ		ㅂ ㅅ ㅆ

Table 5: Results from the zero-shot task to predict 'rounded' consonants using LSTM embeddings. Using a classifier to predict the vowel roundness of consonants, the following consonants are retrieved. F1 score indicates the ability to identify consonants with a labial place of articulation.

tives being voiceless, and plosives being the majority class), the task captured by the classifier may be distorted. The fact that the classifier may not be able to pick up features of voiceness from the Korean embeddings are reflected in the zero-shot experiment.

The results for the first zero-shot experiment for predicting vowels using the classifier for identifying voiced consonants are found in Table 4. Here, the results for Korean are worse than the random baseline. While the results for English and Dutch can be explained by the most-frequent strategy, the result for Spanish indicates that features of voiceness or sonority are encoded in the embeddings, amplifying the initial results from the probing classifier experiment.

Turning from consonant to vowel features, the inventory of vowels is considerably smaller, leaving a small number of training examples with few positive examples. Thus, the F1 scores for the probing classifiers are associated with great uncertainty. Table 5 shows the results for the zero-shot task of retrieving consonants with labial features from a classifier trained to predict vowel roundness. While the classifier trained on transformer embeddings does not yield any positive examples and is therefore not included in the table, the classifier using LSTM embeddings is able to retrieve labial consonants. While the classifiers from Dutch and Spanish retrieve many false negatives as well, the classifier for Korean only retrieves true positives, but only one of four.

Overall, we believe that the results are promising and a good indication on how character representations can capture features related to phonology. This especially in light of the zero-shot task, that indicates that classifiers are able to transfer knowledge of sonority from embeddings of consonants to unseen vowels.

6 Conclusion

In this work, we attempted to understand the information encoded in character-level representations. We obtained two main types of embeddings: text-based embeddings and perceptual embeddings. While the first type of representations (PPMI, LSTM and transformer) were trained from raw data, perceptual representations were obtained from different sources, such as pronunciation dictionaries, synesthesia data and shape visualizations. We have performed correlation studies between these types for five different languages. Besides, we defined and trained models to predict certain phonological distinctive features in order to interpret the embeddings.

We found interesting patterns in the correlation analysis as a simple first approach for intrinsic character embedding evaluation. While clearly outperforming a random baseline in most cases, the strength of the correlations vary between scripts. For instance, the strong correlation between Korean character embeddings and shape representations provides positive evidence of the suitability of this approach. Further research is required to dissect the differences between character LMs: While the LSTM embeddings showed better correlation with color, the transformer embeddings were superior when compared to sound representations. The inclusion of additional languages and scripts will be helpful to identify more generalizable insights.

The phonological probing tasks show promising results, especially with respect to interpretability. In future work, we will focus on the development of more sophisticated probing tasks, for instance, using contextualized character embeddings or multitask networks with shared layers across tasks.

Finally, we stress the need for further intrinsic evaluation methods for character representations. The high impact of orthography on human language learning is an adamant argument to consider the cross-linguistic diversity of writing systems more carefully in the development of NLP models.

578
579
580
581
582
583
584
585

586
587
588
589

590
591
592
593
594

595
596
597
598
599

600
601
602
603
604

605
606
607
608

609
610
611
612

613
614
615
616
617

618
619
620
621

622
623
624
625
626
627
628

629
630
631
632
633

References

Wafia Adouane, Simon Dobnik, Jean-Philippe Bernardy, and Nasredine Semmar. 2018. A comparison of character neural language model and bootstrapping for language identification in multilingual noisy texts. In *Proceedings of the Second Workshop on Subword/Character Level Models*, pages 22–31.

SungMahn Ahn, Yeojin Chung, Jaejoon Lee, and Jiheon Yang. 2017. Korean sentence generation using phoneme-level lstm language model. *Journal of Intelligence and Information Systems*, 23(2):71–88.

Rami Al-Rfou, Dokook Choe, Noah Constant, Mandy Guo, and Llion Jones. 2019. Character-level language modeling with deeper self-attention. In *Proceedings of the AAAI Conference on Artificial Intelligence*, volume 33, pages 3159–3166.

Emily M Bender. 2018. How to make ends meet: Why general purpose NLU needs linguistics. In *Talk presented at the Workshop on Relevance of Linguistic Structure in Neural Architectures for NLP (RELNLP) at ACL*.

David Brang, Romke Rouw, Vilayanur S Ramachandran, and Seana Coulson. 2011. Similarly shaped letters evoke similar colors in grapheme–color synesthesia. *Neuropsychologia*, 49(5):1355–1358. Publisher: Elsevier.

Xinxiong Chen, Lei Xu, Zhiyuan Liu, Maosong Sun, and Huanbo Luan. 2015. Joint learning of character and word embeddings. In *Twenty-Fourth International Joint Conference on Artificial Intelligence*.

Jonathan H Clark, Dan Garrette, Iulia Turc, and John Wieting. 2021. Canine: Pre-training an efficient tokenization-free encoder for language representation. *arXiv preprint arXiv:2103.06874*.

Pierre Courrieu, Fernand Farioli, and Jonathan Grainger. 2004. Inverse discrimination time as a perceptual distance for alphabetic characters. *Visual Cognition*, 11(7):901–919. Publisher: Taylor & Francis.

David M Eagleman, Arielle D Kagan, Stephanie S Nelson, Deepak Sagaram, and Anand K Sarma. 2007. A standardized test battery for the study of synesthesia. *Journal of neuroscience methods*, 159(1):139–145.

Manaal Faruqui, Yulia Tsvetkov, Graham Neubig, and Chris Dyer. 2016. Morphological Inflection Generation Using Character Sequence to Sequence Learning. In *Proceedings of the 2016 Conference of the North American Chapter of the Association for Computational Linguistics: Human Language Technologies*, pages 634–643.

Ram Frost, Leonard Katz, and Shlomo Bentin. 1987. Strategies for visual word recognition and orthographical depth: a multilingual comparison. *Journal of Experimental Psychology: Human Perception and Performance*, 13(1):104.

James S Gale. 1912. The korean alphabet. *Transactions of the Korea Branch of the Royal Asiatic Society*, 4(Part 1). 634
635
636

Eleanor Jack Gibson. 1969. Principles of perceptual learning and development. Publisher: Appleton-Century-Crofts. 637
638
639

Leilani H Gilpin, David Bau, Ben Z Yuan, Ayesha Bajwa, Michael Specter, and Lalana Kagal. 2018. Explaining explanations: An overview of interpretability of machine learning. In *2018 IEEE 5th International Conference on data science and advanced analytics (DSAA)*, pages 80–89. IEEE. 640
641
642
643
644
645

Kyle Gorman, Lucas F.E. Ashby, Aaron Goyzueta, Arya McCarthy, Shijie Wu, and Daniel You. 2020. The SIGMORPHON 2020 shared task on multilingual grapheme-to-phoneme conversion. In *Proceedings of the 17th SIGMORPHON Workshop on Computational Research in Phonetics, Phonology, and Morphology*, pages 40–50, Online. Association for Computational Linguistics. 646
647
648
649
650
651
652
653

Mandy Guo, Zihang Dai, Denny Vrandečić, and Rami Al-Rfou. 2020. Wiki-40B: Multilingual language model dataset. In *Proceedings of the 12th Language Resources and Evaluation Conference*, pages 2440–2452, Marseille, France. European Language Resources Association. 654
655
656
657
658
659

Ximena Gutierrez-Vasques, Christian Bentz, Olga Sozinova, and Tanja Samardzic. 2021. From characters to words: the turning point of BPE merges. In *Proceedings of the 16th Conference of the European Chapter of the Association for Computational Linguistics: Main Volume*, pages 3454–3468, Online. Association for Computational Linguistics. 660
661
662
663
664
665
666

Ximena Gutierrez-Vasques and Victor Mijangos. 2020. Productivity and predictability for measuring morphological complexity. *Entropy*, 22(1):48. 667
668
669

Sittichai Jiampojarn, Grzegorz Kondrak, and Tarek Sherif. 2007. Applying many-to-many alignments and hidden markov models to letter-to-phoneme conversion. In *Human Language Technologies 2007: The Conference of the North American Chapter of the Association for Computational Linguistics; Proceedings of the Main Conference*, pages 372–379, Rochester, New York. Association for Computational Linguistics. 670
671
672
673
674
675
676
677
678

Katharina Kann, Samuel R Bowman, and Kyunghyun Cho. 2020. Learning to learn morphological inflection for resource-poor languages. In *Proceedings of the AAAI Conference on Artificial Intelligence*, volume 34, pages 8058–8065. Issue: 05. 679
680
681
682
683

Katharina Kann and Mauro M. Monsalve-Mercado. 2021. Coloring the black box: What synesthesia tells us about character embeddings. In *Proceedings of the 16th Conference of the European Chapter of the Association for Computational Linguistics: Main Volume*, pages 2673–2685, Online. Association for Computational Linguistics. 684
685
686
687
688
689
690

691	Katharina Kann and Hinrich Schütze. 2016. MED: The LMU system for the SIGMORPHON 2016 shared task on morphological reinflection. In <i>Proceedings of the 14th SIGMORPHON Workshop on Computational Research in Phonetics, Phonology, and Morphology</i> , pages 62–70.		
692			
693			
694			
695			
696			
697	Leonard Katz and Ram Frost. 1992. The reading process is different for different orthographies: The Orthographic Depth Hypothesis. In <i>Advances in psychology</i> , volume 94, pages 67–84. Elsevier.		
698			
699			
700			
701	Yoon Kim, Yacine Jernite, David Sontag, and Alexander M Rush. 2016. Character-aware neural language models. In <i>30th AAAI Conference on Artificial Intelligence, AAAI 2016</i> , pages 2741–2749. AAAI press.		
702			
703			
704			
705	Diederik P. Kingma and Jimmy Ba. 2015. Adam: A method for stochastic optimization. In <i>3rd International Conference on Learning Representations, ICLR 2015, San Diego, CA, USA, May 7-9, 2015, Conference Track Proceedings</i> .		
706			
707			
708			
709			
710	Sudheer Kolachina and Lilla Magyar. 2019. What do phone embeddings learn about phonology? In <i>Proceedings of the 16th Workshop on Computational Research in Phonetics, Phonology, and Morphology</i> , pages 160–169, Florence, Italy. Association for Computational Linguistics.		
711			
712			
713			
714			
715			
716	Guillaume Lample, Miguel Ballesteros, Sandeep Subramanian, Kazuya Kawakami, and Chris Dyer. 2016. Neural Architectures for Named Entity Recognition. In <i>Proceedings of the 2016 Conference of the North American Chapter of the Association for Computational Linguistics: Human Language Technologies</i> , pages 260–270.		
717			
718			
719			
720			
721			
722			
723	Karin Landerl, Franck Ramus, Kristina Moll, Heikki Lyytinen, Paavo HT Leppänen, Kaisa Lohvan- suu, Michael O’Donovan, Julie Williams, Jürgen Bartling, Jennifer Bruder, et al. 2013. Predictors of developmental dyslexia in european orthographies with varying complexity. <i>Journal of Child Psychol- ogy and Psychiatry</i> , 54(6):686–694.		
724			
725			
726			
727			
728			
729			
730	Jackson L. Lee, Lucas F.E. Ashby, M. Elizabeth Garza, Yeonju Lee-Sikka, Sean Miller, Alan Wong, Arya D. McCarthy, and Kyle Gorman. 2020a. Massively multilingual pronunciation modeling with WikiPron. In <i>Proceedings of the 12th Language Resources and Evaluation Conference</i> , pages 4223–4228, Mar- seille, France. European Language Resources Asso- ciation.		
731			
732			
733			
734			
735			
736			
737			
738	Sang-Oak Lee. 2021. 5. graphical ingenuity in the ko- rean writing system: With new reference to calligra- phy. In <i>The Korean alphabet</i> , pages 107–116. Uni- versity of Hawaii Press.		
739			
740			
741			
742	Sangah Lee, Hansol Jang, Yunmee Baik, Suzi Park, and Hyopil Shin. 2020b. Kr-bert: A small-scale korean-specific language model. <i>arXiv preprint arXiv:2008.03979</i> .		
743			
744			
745			
	Yanran Li, Wenjie Li, Fei Sun, and Sujian Li. 2015. Component-enhanced chinese character embeddings. In <i>Proceedings of the 2015 Conference on Empirical Methods in Natural Language Processing</i> , pages 829–834.	746	747
		748	749
		750	
	Wang Ling, Chris Dyer, Alan W Black, Isabel Trancoso, Ramón Fernandez, Silvio Amir, Luis Marujo, and Tiago Luís. 2015. Finding Function in Form: Compositional Character Models for Open Vocabulary Word Representation. In <i>Proceedings of the 2015 Conference on Empirical Methods in Natural Language Processing</i> , pages 1520–1530.	751	752
		753	754
		755	756
		757	
	Wentao Ma, Yiming Cui, Chenglei Si, Ting Liu, Shijin Wang, and Guoping Hu. 2020. CharBERT: Character-aware pre-trained language model. In <i>Proceedings of the 28th International Conference on Computational Linguistics</i> , pages 39–50, Barcelona, Spain (Online). International Committee on Computational Linguistics.	758	759
		760	761
		762	763
		764	
	Xavier Marjou. 2021. OTEANN: Estimating the transparency of orthographies with an artificial neural network. In <i>Proceedings of the Third Workshop on Computational Typology and Multilingual NLP</i> , pages 1–9, Online. Association for Computational Linguistics.	765	766
		767	768
		769	770
	Connor Mayer. 2020. An algorithm for learning phonological classes from distributional similarity. <i>Phonology</i> , 37(1):91–131.	771	772
		773	
	Connor Mayer and Max Nelson. 2020. Phonotactic learning with neural language models. <i>Proceedings of the Society for Computation in Linguistics</i> , 3(1):149–159.	774	775
		776	777
	Sabrina J Mielke, Ryan Cotterell, Kyle Gorman, Brian Roark, and Jason Eisner. 2019. What kind of language is hard to language-model? In <i>Proceedings of the 57th Annual Meeting of the Association for Computational Linguistics</i> , pages 4975–4989.	778	779
		780	781
		782	
	Nicole Mirea and Klinton Bicknell. 2019. Using LSTMs to assess the obligatoriness of phonological distinctive features for phonotactic learning. In <i>Proceedings of the 57th Annual Meeting of the Association for Computational Linguistics</i> , pages 1595–1605, Florence, Italy. Association for Computational Linguistics.	783	784
		785	786
		787	788
		789	
	Shotaro Misawa, Motoki Taniguchi, Yasuhide Miura, and Tomoko Ohkuma. 2017. Character-based bidirectional lstm-crf with words and characters for japanese named entity recognition. In <i>Proceedings of the first workshop on subword and character level models in NLP</i> , pages 97–102.	790	791
		792	793
		794	795
	Thi-Vinh Ngo, Thanh-Le Ha, Phuong-Thai Nguyen, and Le-Minh Nguyen. 2019. How transformer revitalizes character-based neural machine translation: An investigation on japanese-vietnamese translation systems. <i>arXiv preprint arXiv:1910.02238</i> .	796	797
		798	799
		800	

801	Viet Nguyen, Julian Brooke, and Timothy Baldwin.	857
802	2017. Sub-character neural language modelling in	858
803	japanese. In <i>Proceedings of the first workshop on</i>	859
804	<i>subword and character level models in NLP</i> , pages	860
805	148–153.	
806	Byung-Doh Oh, Christian Clark, and William Schuler.	861
807	2021. Surprisal estimators for human reading times	862
808	need character models. In <i>Proceedings of the 59th</i>	863
809	<i>Annual Meeting of the Association for Computa-</i>	864
810	<i>tional Linguistics and the 11th International Joint</i>	865
811	<i>Conference on Natural Language Processing (Vol-</i>	866
812	<i>ume 1: Long Papers)</i> .	867
813	Timothy C Papadopoulos, Valéria Csépe, Mikko	868
814	Aro, Marketa Caravolas, Irene-Anna Diakidoy, and	869
815	Thierry Olive. 2021. Methodological issues in liter-	870
816	acy research across languages: Evidence from alpha-	871
817	betic orthographies. <i>Reading Research Quarterly</i> ,	
818	56:S351–S370.	
819	Sungjoon Park, Jeongmin Byun, Sion Baek, Yongseok	
820	Cho, and Alice Oh. 2018. Subword-level word vec-	
821	tor representations for korean. In <i>Proceedings of the</i>	
822	<i>56th Annual Meeting of the Association for Compu-</i>	
823	<i>tational Linguistics (Volume 1: Long Papers)</i> , pages	
824	2429–2438.	
825	Fabio Richlan. 2020. The functional neuroanatomy of	
826	developmental dyslexia across languages and writ-	
827	ing systems. <i>Frontiers in psychology</i> , 11:155.	
828	Nicholas B Root, Romke Rouw, Michiko Asano, Chai-	
829	Youn Kim, Helena Melero, Kazuhiko Yokosawa,	
830	and Vilayanur S Ramachandran. 2018. Why is the	
831	synesthete’s “A” red? Using a five-language dataset	
832	to disentangle the effects of shape, sound, semantics,	
833	and ordinality on inducer–concurrent relationships	
834	in grapheme-color synesthesia. <i>cortex</i> , 99:375–389.	
835	D. E. Rumelhart and J. L. McClelland. 1986. <i>On Learn-</i>	
836	<i>ing the Past Tenses of English Verbs</i> , page 216–271.	
837	MIT Press, Cambridge, MA, USA.	
838	Geoffrey. Sampson. 1985. <i>Writing systems : a linguis-</i>	
839	<i>tic introduction</i> . Hutchinson, London.	
840	Geoffrey Sampson. 1990. The writing systems of the	
841	world. <i>Journal of Linguistics</i> , 26(1):275–276.	
842	Xenia Schmalz, Eva Marinus, Max Coltheart, and	
843	Anne Castles. 2015. Getting to the bottom of or-	
844	thographic depth. <i>Psychonomic bulletin & review</i> ,	
845	22(6):1614–1629.	
846	Rico Sennrich, Barry Haddow, and Alexandra Birch.	
847	2016. Neural Machine Translation of Rare Words	
848	with Subword Units. In <i>Proceedings of the 54th An-</i>	
849	<i>nuual Meeting of the Association for Computational</i>	
850	<i>Linguistics (Volume 1: Long Papers)</i> , pages 1715–	
851	1725.	
852	Philip HK Seymour, Mikko Aro, Jane M Erskine,	
853	and Collaboration with COST Action A8 Network.	
854	2003. Foundation literacy acquisition in euro-	
855	pean orthographies. <i>British Journal of psychology</i> ,	
856	94(2):143–174.	
	David L Share. 2008. On the anglocentricities of cur-	857
	rent reading research and practice: The perils of over-	858
	reliance on an “outlier” orthography. <i>Psychological</i>	859
	<i>Bulletin</i> , 134(4):584.	860
	Miikka Silfverberg, Francis Tyers, Garrett Nicolai, and	861
	Mans Hulden. 2021. Do RNN states encode abstract	862
	phonological alternations? In <i>Proceedings of the</i>	863
	<i>2021 Conference of the North American Chapter of</i>	864
	<i>the Association for Computational Linguistics: Hu-</i>	865
	<i>man Language Technologies</i> , pages 5501–5513, On-	866
	line. Association for Computational Linguistics.	867
	Miikka P. Silfverberg, Lingshuang Mao, and Mans	868
	Hulden. 2018. Sound analogies with phoneme em-	869
	beddings . In <i>Proceedings of the Society for Compu-</i>	870
	<i>tation in Linguistics (SCiL) 2018</i> , pages 136–144.	871
	Richard Sproat and Alexander Gutkin. 2021. The Tax-	872
	onomy of Writing Systems: How to Measure How	873
	Logographic a System Is . <i>Computational Linguis-</i>	874
	<i>tics</i> , 47(3):477–528.	875
	Karl Stratos. 2017. A sub-character architecture for	876
	korean language processing. In <i>Proceedings of the</i>	877
	<i>2017 Conference on Empirical Methods in Natural</i>	878
	<i>Language Processing</i> , pages 721–726.	879
	Sho Takase, Jun Suzuki, and Masaaki Nagata. 2019.	880
	Character n-gram embeddings to improve rnn lan-	881
	guage models. In <i>Proceedings of the AAAI Con-</i>	882
	<i>ference on Artificial Intelligence</i> , volume 33, pages	883
	5074–5082.	884
	Yi Tay, Vinh Q Tran, Sebastian Ruder, Jai Gupta,	885
	Hyung Won Chung, Dara Bahri, Zhen Qin, Si-	886
	mon Baumgartner, Cong Yu, and Donald Metzler.	887
	2021. Charformer: Fast character transformers	888
	via gradient-based subword tokenization. <i>arXiv</i>	889
	<i>preprint arXiv:2106.12672</i> .	890
	Ashish Vaswani, Noam Shazeer, Niki Parmar, Jakob	891
	Uszkoreit, Llion Jones, Aidan N Gomez, Łukasz	892
	Kaiser, and Illia Polosukhin. 2017. Attention is all	893
	you need. In <i>Advances in neural information pro-</i>	894
	<i>cessing systems</i> , pages 5998–6008.	895
	Marcus R Watson, Kathleen A Akins, and	896
	James T Enns. 2012. Second-order mappings	897
	in grapheme–color synesthesia . <i>Psychonomic</i>	898
	<i>Bulletin & Review</i> , 19(2):211–217. Publisher:	899
	Springer.	900
	Johannes C Ziegler, Daisy Bertrand, Dénes Tóth,	901
	Valéria Csépe, Alexandra Reis, Luís Faísca, Nina	902
	Saine, Heikki Lyytinen, Anniek Vaessen, and Leo	903
	Blomert. 2010. Orthographic depth and its impact	904
	on universal predictors of reading: A cross-language	905
	investigation. <i>Psychological science</i> , 21(4):551–	906
	559.	907

A Preprocessing

We download the Wiki40B dataset for each of the five languages (English, Dutch, Japanese, Korean, and Spanish) from TensorFlow Hub⁴. For English and Dutch, we consider the 26 standard letters of the alphabet, digits and punctuation marks. For Spanish, we additionally add \tilde{n} and remove diacritics from vowels. For Korean, we consider all Hangeul characters, digits and punctuation marks. Since Hangeul is a featural writing system (Sampson, 1990), we split the Jamos (i.e., compound symbols) into syllables⁵. For Japanese, we consider all Hiragana, Katakana, and Kanji characters for training the language model. However, for subsequent analyses we focus only on Hiragana. For all languages, we replace any other special characters with the symbol €.

B Datasets

B.1 Sound embeddings

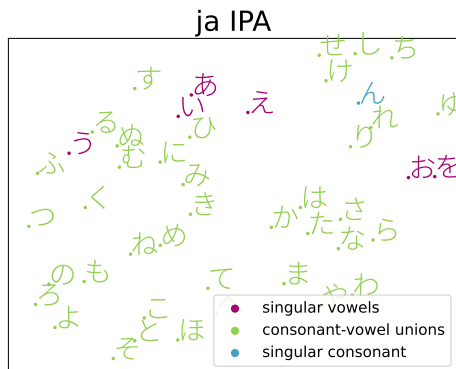


Figure 4: Japanese sound embeddings.

B.2 Synesthesia Dataset

As described in the main paper, we use the synesthesia data collected by Root et al. 2018. The data is available upon request by the first author. Table 6 shows the number of characters and participants included for each language in the dataset.

In Figure 5 the characters are plotted by the distances between their corresponding colors. Based on this dataset, Root et al. 2018 showed how some influences on grapheme-color associations in synesthesia might be universal across languages. Their

⁴<https://www.tensorflow.org/datasets/catalog/wiki40b>

⁵<https://pypi.org/project/jamotools/>

Language	# Chars	# Participants
English	26	47
Dutch	26	110
Japanese	46	27
Korean	24	13
Spanish	26	32

Table 6: Synesthesia dataset details showing the number of characters included for each language and the number of synesthetes participating in the study.

results suggest that grapheme-color associations follow an ordinal explanation, meaning that the unusually-distrinct first grapheme of a synesthete’s alphabet tends to be associated with the unsuluayy-distinct color red. In line with their findings, the clusters show the greatest distance between the associated colors of the first grapheme of the alphabets (i.e., "a" in English and Spanish and "ㅏ" in Korean).

B.3 Shape Dataset

Please find in figure 7 some examples of character figures that were used to build shape representations. We besides include in figure 8 three dendrograms calculated from the shape representations. For Spanish, English, and Dutch we only calculated one dendrogram, as the only difference is that the Spanish alphabet contains the “ñ” letter. For Japanese, we show a random subset (50%) of the *Hiragana* alphabet, as it did not fit properly in our plots.

C Models

C.1 Training Procedure

For the LSTM, biLSTM and transformer models, the number of epochs is set to 100, but the models are trained with early stopping and training is ended after 3 epochs without improvement on the validation loss. The best model is saved and used to extract the character embeddings. For reproducibility purposes, we set a single random seed.

967 **D Grapheme-to-phoneme alignments**

968 **D.1 Dutch**

969 a:a, b:b, c:k, d:d, e:ε, f:f, g:y, h:fi, i:, j:j, k:k, l:l,
970 m:m, n:n, o:ɔ, p:p, r:r, s:s, t:t, u:œy, v:v, w:u,
971 x:ks, z:z, q:k, y:j

972 **D.2 English**

973 a:æ, b:b, c:k, d:d, e:ε, f:f, g:, h:h, i:, j:ʤ, k:k,
974 l:l, m:m, n:n, o:ɒ, p:p, q:k, r:ɹ, s:s, t:t, u:ʌ, v:v,
975 w:w, x:z, y:j, z:z

976 **D.3 Korean**

977 ㅅ:s, ㅇ:j, ㅈ:ㄸ, ㅊ:ㅉ, ㅋ:ㅋ, ㆁ:ㅇ, ㄷ:ㄷ,
978 ㅌ:ㄹ, ㅍ:ㅍ, ㅑ:k, ㅓ:n, ㅕ:t, ㅗ:ㅜ,
979 ㅛ:r, ㅜ:m, ㅝ:p, ㅞ:p, ㅟ:ㅠ, ㅡ:ㅢ,
980 k^h, ㅣ:t^h, ㅤ:p^h, ㅎ:h, :n, :m, :,

981 **D.4 Spanish**

982 a:a, b:b, c:k, d:d, e:e, f:f, g:, h:x, i:i, j:x, k:k
983 , l:l, m:m, n:n, o:o, p:p, q:k, r:r, s:s, t:t, u:u,
984 v:b, w:w, x:s, y:ʝ, z:θ

985 **E Probing Task**

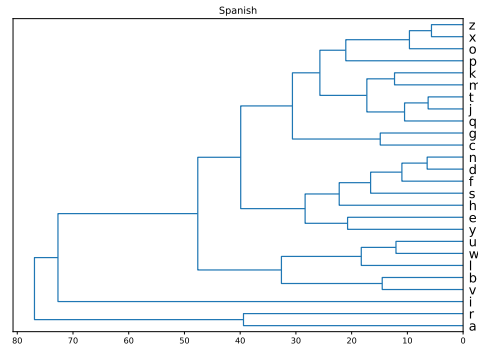
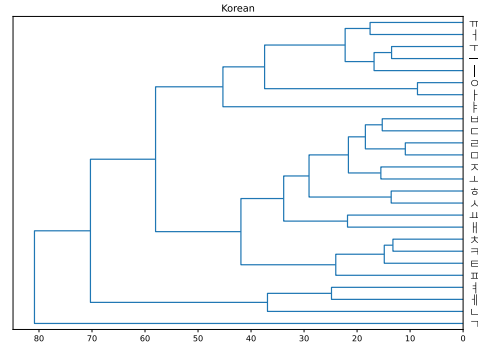
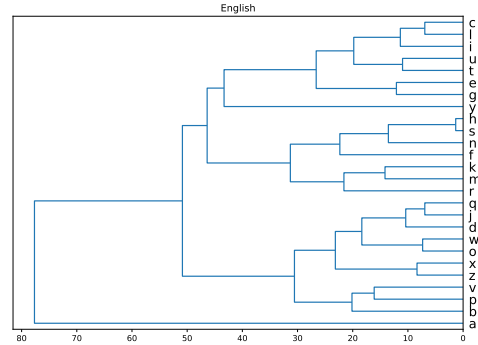


Figure 5: Dendrograms of the distances between colors assigned to each character for English, Korean and Spanish. The leaves are sorted so that the minimum distance between its direct descendants is plotted first.

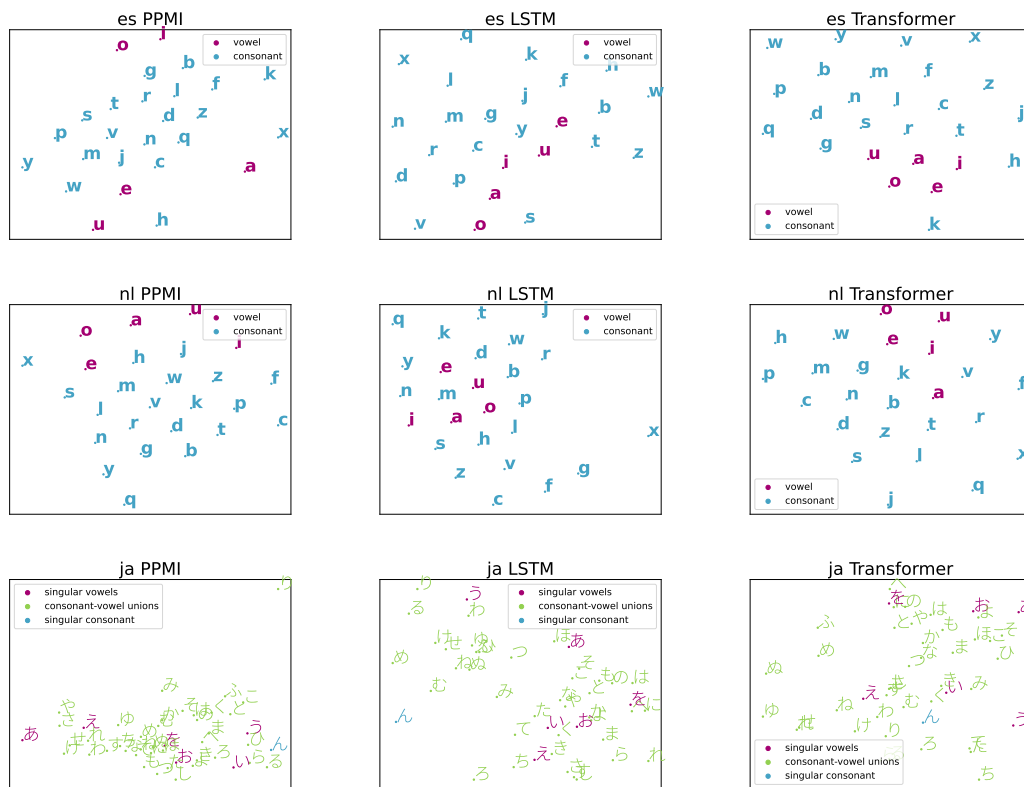


Figure 6: tSNE cluster plots of the three types of character models for Spanish, Dutch and Japanese.

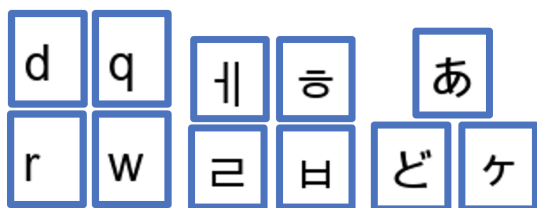


Figure 7: Example images from which we extract character shape representations from the Latin alphabets, the Korean *Hangul* alphabet and the Japanese *Hiragana* alphabet.

Model		global type		consonant voiceness	
		<i>consonant</i>	<i>vowel</i>	<i>voiced</i>	<i>voiceless</i>
en	LSTM	0.84	0.22	0.67	0.17
	Transformer	0.90	0.60	0.86	0.71
	Random	0.61	0.28	0.54	0.43
	Most-frequent	0.89	0.00	0.76	0.00
es	LSTM	0.91	0.50	0.57	0.61
	Transformer	0.98	0.89	0.72	0.63
	Random	0.61	0.27	0.49	0.49
	Most-frequent	0.90	0.00	0.00	0.00
ko	LSTM	1.00	1.00	0.00	0.88
	Transformer	1.00	1.00	0.33	0.87
	Random	0.59	0.35	0.29	0.60
	Most-frequent	0.84	0.00	0.00	0.88
nl	LSTM	0.91	0.50	0.62	0.15
	Transformer	0.93	0.67	0.79	0.57
	Random	0.61	0.28	0.54	0.42
	Most-frequent	0.89	0.00	0.76	0.00

Model		consonant place					
		<i>alveolar</i>	<i>alveolo-palatal</i>	<i>bilabial</i>	<i>labio-dental</i>	<i>palatal</i>	<i>velar</i>
en	LSTM	0.63	-	0.00	0.00	-	0.40
	Transformer	0.38	-	0.00	0.00	-	0.00
	Random	0.46	-	0.22	0.16	-	0.27
	Most-frequent	0.00	-	0.00	0.00	-	0.00
es	LSTM	0.36	-	0.00	-	0.00	0.17
	Transformer	0.62	-	0.00	-	0.00	0.00
	Random	0.38	-	0.26	-	0.15	0.35
	Most-frequent	0.00	-	0.00	-	0.00	0.00
ko	LSTM	0.33	0.00	0.00	-	-	0.00
	Transformer	0.40	0.00	0.00	-	-	0.00
	Random	0.49	0.23	0.29	-	-	0.23
	Most-frequent	0.00	0.00	0.00	-	-	0.00
nl	LSTM	0.14	-	0.00	0.00	0.00	0.29
	Transformer	0.77	-	0.00	0.00	0.00	0.33
	Random	0.43	-	0.22	0.23	0.16	0.32
	Most-frequent	0.00	-	0.00	0.00	0.00	0.00

Model		consonant manner				
		<i>approximant</i>	<i>nasal</i>	<i>non-sibilant-fricative</i>	<i>plosive</i>	<i>sibilant-fricative</i>
en	LSTM	0.00	0.00	0.00	0.35	0.40
	Transformer	0.00	0.00	0.00	0.59	0.00
	Random	0.23	0.16	0.22	0.45	0.27
	Most-frequent	0.00	0.00	0.00	0.00	0.00
es	LSTM	-	0.50	0.00	0.30	0.00
	Transformer	-	0.00	0.00	0.53	0.00
	Random	-	0.21	0.26	0.45	0.15
	Most-frequent	-	0.00	0.00	0.00	0.00
ko	LSTM	-	0.00	-	0.52	0.00
	Transformer	-	0.00	-	0.73	0.00
	Random	-	0.17	-	0.53	0.30
	Most-frequent	-	0.00	-	0.73	0.00
nl	LSTM	0.00	0.00	0.57	0.33	0.00
	Transformer	0.00	0.00	0.00	0.25	0.00
	Random	0.22	0.16	0.28	0.42	0.22
	Most-frequent	0.00	0.00	0.00	0.00	0.00

Model		vowel height				vowel backness		vowel roundness	
		<i>close</i>	<i>close-mid</i>	<i>mid</i>	<i>open-mid</i>	<i>front</i>	<i>back</i>	<i>rounded</i>	<i>unrounded</i>
en	LSTM	-	-	-	0.00	0.00	0.00	-	-
	Transformer	-	-	-	0.00	0.00	0.00	-	-
	Random	-	-	-	0.42	0.41	0.42	-	-
	Most-frequent	-	-	-	0.00	0.00	0.00	-	-
es	LSTM	0.00	0.00	-	-	0.57	0.00	0.00	0.57
	Transformer	0.00	0.00	-	-	0.33	0.00	0.00	0.33
	Random	0.41	0.42	-	-	0.50	0.42	0.43	0.49
	Most-frequent	0.00	0.00	-	-	0.00	0.00	0.00	0.00
ko	LSTM	0.00	-	0.00	-	0.00	0.25	0.00	0.83
	Transformer	0.00	-	0.00	-	0.00	0.00	0.00	0.83
	Random	0.45	-	0.35	-	0.35	0.52	0.35	0.56
	Most-frequent	0.00	-	0.00	-	0.00	0.00	0.00	0.83
nl	LSTM	-	-	-	0.00	0.00	0.00	0.00	0.33
	Transformer	-	-	-	0.57	0.00	0.00	0.00	0.57
	Random	-	-	-	0.51	0.41	0.42	0.43	0.51
	Most-frequent	-	-	-	0.00	0.00	0.00	0.00	0.00

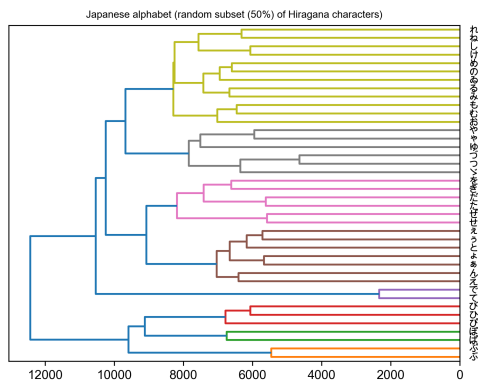
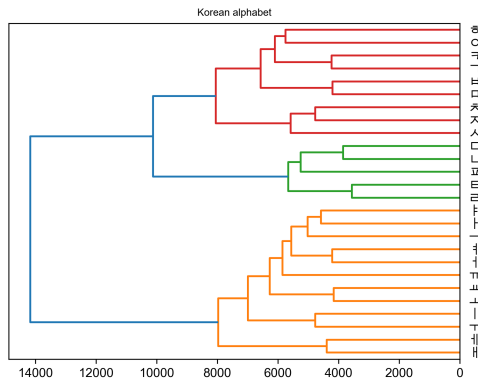
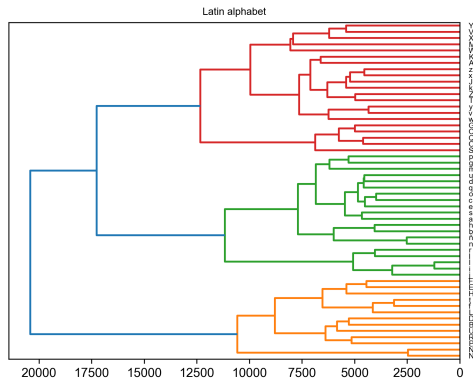


Figure 8: Dendrograms of the distances between shape representations for the Latin alphabet (including the Spanish ñ letter), Korean *Hangul* alphabet and a subset of the Japanese *Hiragana* alphabet.